Chin. Geogra. Sci. 2020 Vol. 30 No. 2 pp. 266–278
https://doi.org/10.1007/s11769-020-1110-7

Springer Science Press
www.springerlink.com/content/1002-0063

Inventory of Atmospheric Pollutant Emissions from Burning of Crop Residues in China Based on Satellite-retrieved Farmland Data

LI Ruimin[1, 2], CHEN Weiwei[1], ZHAO Hongmei[1], WU Xuewei[1, 2], ZHANG Mengduo[1, 2], TONG Daniel Q[3, 4], XIU Aijun[1]

(1. *Key Laboratory of Wetland Ecology and Environment*, *Northeast Institute of Geography and Agroecology*, *Chinese Academy of Sciences*, *Changchun* 130102, *China*; 2. *University of Chinese Academy of Sciences*, *Beijing* 100049, *China*; 3. *Center for Spatial Information Science and Systems*, *George Mason University*, *Fairfax VA* 22030, *USA*; 4. *Cooperative Institute for Climate & Satellites*, *University of Maryland*, *MD* 20740, *USA*)

Abstract: The burning of crop residues emits large quantities of atmospheric aerosols. Published studies have developed inventories of emissions from crop residue burning based on statistical data. In contrast, this study used satellite-retrieved land-cover data (1 km × 1 km) as activity data to compile an inventory of atmospheric pollutants emitted from the burning of crop residues in China in 2015. The emissions of PM_{10}, $PM_{2.5}$, VOCs, NO_x, SO_2, CO, and NH_3 from burning crop straw on nonirrigated farmland in China in 2015 were 610.5, 598.4, 584.4, 230.6, 35.4, 3329.3, and 36.1 Gg (1 Gg = 10^9 g), respectively; the corresponding emissions from burning paddy rice residues were 234.1, 229.7, 342.3, 57.5, 57.5, 1122.1, and 21.5 Gg, respectively. The emissions from crop residue burning showed large spatial and temporal variations. The emissions of particulate matter and gaseous pollutants from crop residue burning in nonirrigated farmland were highest in east China, particularly in Shandong, Henan, Anhui, and Sichuan provinces. Emissions from burning paddy rice residue were highest in east and central China, with particularly high levels in Shandong, Jiangsu, Zhejiang, and Hunan provinces. The monthly variations in atmospheric pollutant emissions were similar among different regions, with the highest levels observed in October in north, northeast, northwest, east, and southwest China and in June and July in central and south China. The developed inventory of emissions from crop residue burning is expected to help improve air quality models by providing high-resolution spatial and temporal data.

Keywords: crop residue burning; land-cover data; particular matter (PM); gaseous pollutants; emission inventory

Citation: LI Ruimin, CHEN Weiwei, ZHAO Hongmei, WU Xuewei, ZHANG Mengduo, TONG Daniel Q, XIU Aijun, 2020. Inventory of Atmospheric Pollutant Emissions from Burning of Crop Residues in China Based on Satellite-retrieved Farmland Data. *Chinese Geographical Science*, 30(2): 266–278. https://doi.org/10.1007/s11769-020-1110-7

1 Introduction

China is one of the leading crop-producing countries, with a total grain production of 62 143.9 × 10^4 t in 2015 (NBSC, 2016a). This large crop production coupled with a lack of effective emission control strategies for open biomass burning leads to the large-scale burning of crop straw in open fields during the harvest period. Previous studies have confirmed that crop residue burning contributes to the emission of large quantities of atmospheric pollutants (Zhang et al., 2006; 2009; Wang and Zhang, 2008; He et al., 2013; Zhou et al., 2017). An ac-

Received date: 2019-05-08; accepted date: 2019-09-02
Foundation item: Under the auspices of National Key R & D Program of China (No. 2017YFC0212303, 2017YFC0212304), Key Research Program of Frontier Sciences, Chinese Academy of Sciences (No. QYZDB-SSW-DQC045), National Natural Science Foundation of China (No. 41775116), Youth Innovation Promotion Association of Chinese Academy of Sciences (No. 2017275)
Corresponding author: CHEN Weiwei. E-mail: chenweiwei@iga.ac.cn; ZHAO Hongmei. E-mail: zhaohongmei@iga.ac.cn

curate inventory of atmospheric pollutants emitted by crop residue burning is necessary to understand, predict, and control the effects of agricultural emissions on air quality and human health.

Published studies have estimated the emissions of atmospheric pollutants from crop residue burning using both bottom-up and top-down methods. Several studies have developed inventories of atmospheric pollutants emitted by crop residue burning based on statistical yearbook data, which generally have province- or city-level resolution (Wang and Zhang., 2008; Peng et al., 2016). County-level pollutant emission inventories are difficult to develop because detailed data can not be obtained directly from statistical yearbooks (Zhou et al., 2017). Emission inventories developed using statistical data have lower resolutions than those based on fire count data from satellite observations. In the top-down method, fire count data are used to determine the temporal and spatial distributions of fire-related emissions. This method can reduce the uncertainty in the estimated emissions of atmospheric pollutants. However, inventories of emissions from crop residue burning tend to have large uncertainty due to the lack of localized vegetation data and/or the use of only province-level data of burned cropland area (Qiu et al., 2016; Wu et al., 2018). The emissions inventories that are based on bottom-up or top-down approaches are necessary, due to their performing cross-examinations of the atmospheric pollutant emissions between various agricultural inventories, it was an important method for verifying the accuracy of emission inventories (EEA, 2007).

In this study, we developed a high-resolution inventory of emissions from residual crop burning based on high-resolution land-cover data (1 km × 1 km) from satellite observations and county-level data burned cropland area data. Land-cover data derived from satellite remote sensing observations were used as activity data to quantify the emissions of atmospheric pollutants from crop residue burning in China for the year 2015 and characterize their spatial and temporal distributions. The resulting high-resolution inventory provides a detailed description of emissions from crop residue burning in China. The inventory is expected to improve the accuracy of atmospheric aerosol models and aid the design of national and local policies to control agricultural emissions.

2 Data and Methods

2.1 Study area

The study region, which includes the 27 provinces and four municipalities (Beijing, Tianjin, Shanghai, and Chongqing) of China (except for Hong Kong, Macao and Taiwan of China) ranges from 3°51′N to 53°33′N and 73°33′E to 135°05′E. Spatial variations in emissions are presented with a resolution of 1 km × 1 km in seven regions: north, northwest, east, central, south, southwest, and northwest China (Fig. 1 and Table 1). The spatial distributions of paddy and nonirrigated farmland in China indicate that paddy areas are primarily distributed in east China, south China, central China, Sichuan, and Heilongjiang, while nonirrigated farmland is prevalent in North China, Northwest China, Southwest China, Northeast China, Henan, and Shandong (http://www. resdc.cn/). We developed an inventory of atmospheric pollutant emissions from crop reside burning using a technology-based emission factor method. This emission inventory was developed for China in 2015 based on satellite-retrieved farmland data. The atmospheric pollutants considered were particulate matter (PM_{10} and $PM_{2.5}$) and gaseous pollutants (SO_2, NO_x, CO, VOCs, and NH_3).

2.2 Algorithms for estimating pollutant emissions from crop residue burning

In this section, we describe the method used to estimate emissions from crop residue burning. The method

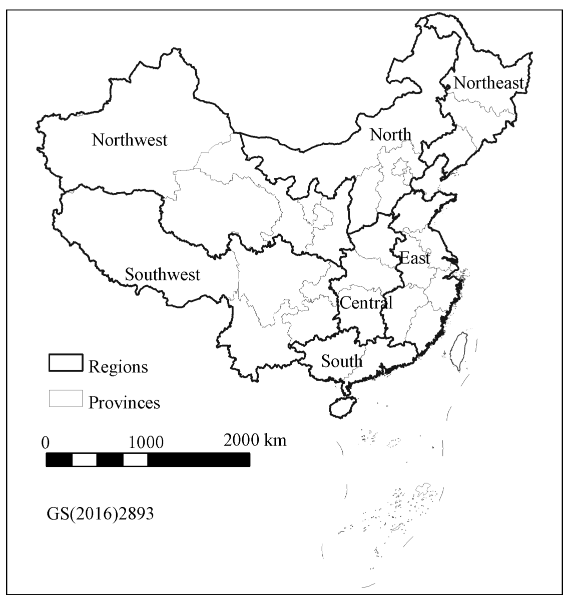

Fig. 1 Study region

employed was derived from 'Technical guidelines on emission inventory development of air pollutants from biomass burning (on trial)' (MEE, 2014) with modification based on the specific activity data used in this study. The emissions of atmospheric pollutants E (g) are given by

$$E=\sum_{i=1}^{M}\sum_{j=1}^{N}\left(A\times P_{i,j}\times Q_{i,j}\times R_i\times B_{i,j}\times EF_i\times F_i\times 100\right) \quad (1)$$

where M is the number of crop types (i), N is the number of grids (j) that represent nonirrigated farmland or paddy regions (land-cover data, 1 km × 1 km), A is the area of the grid (km^2), $P_{i,j}$ is the crop output per area of crop type i in grid j (kg/ha), $Q_{i,j}$ is the percentage of cropland area of crop type i out of all sown areas in grid j (statistical data and county-level data; %), R_i is the ratio of crop residue to production for crop type i (%), $B_{i,j}$ is the percentage of crop straw burned in fields in region j (%), F_i is the combustion efficiency of crop type i (0.9), and EF_i is the emission factor of crop type i (g/kg).

The statistical data for $P_{i,j}$ and $Q_{i,j}$ were collected at the county-level resolution from statistical yearbooks. In the case where county-level activity data ($P_{i,j}$ or $Q_{i,j}$) could not be directly obtained from the yearbook, we calculated county-level crop yield based on the county-level grain yield since grain yield and crop yield are strongly correlated at the prefecture resolution (R = 0.747) (Zhou et al., 2017). The R_i data were based on a questionnaire implemented by Peng et al. (2016). The values of $B_{i,j}$, F_i, and EF_i were obtained according to MEE (2014).

2.3 Activity data

The $P_{i,j}$ data were obtained from the National Bureau of Statistics (http://data.stats.gov.cn/), China Rural Statistical Yearbook (NBSC, 2016a), and the Chinese Statistical Yearbook (NBSC, 2016b). The $Q_{i,j}$ data for each grid (the percentages of crop area out of the total sown area within each county) were obtained from provincial statistical yearbooks (ABS, 2016; BBS, 2016; CBS, 2016; FBS, 2016; GDBS, 2016; GXBS, 2016; GSBS, 2016; GZBS, 2016; HBS, 2016; HBBS, 2016; HNBS, 2016; HUBBS, 2016; HUNBS, 2016; HLJBS, 2016; IMBS, 2016; JSBS, 2016; JXBS, 2016; JLBS, 2016; LBS, 2016; NBS, 2016; QBS, 2016; SBS, 2016; SXBS, 2016; SDBS, 2016; SHBS, 2016; SCBS, 2016; TJBS, 2016; TBS, 2016a; 2016b; XBS, 2016; YBS, 2016; ZBS, 2016), including those of the 27 provinces and four municipalities.

The paddy and nonirrigated farmland areas were extracted from the data of land-cover change in China (remote sensing monitoring data; http://www.resdc.cn/default.aspx) with a resolution of 1 km × 1 km. The 'Raster to points' tool in ArcGIS was used to extract the latitudes and longitudes of the paddy and nonirrigated farmlands. The resulting paddy and nonirrigated farmland areas in 2015 in China are shown in Table 1.

Table 1 Extraction of paddy and nonirrigated farmland areas from the land-cover data of China in 2015

Regions in China	Province	Paddy area (km^2)	Nonirrigated farmland area (km^2)	Regions in China	Province	Paddy area (km^2)	Nonirrigated farmland area (km^2)
North	Beijing	131	4279	Central	Hubei	37744	29507
	Hebei	4538	91141		Hunan	43538	16402
	Inner Mongolia	1209	112766	South	Guangdong	25106	16933
	Shanxi	48	59999		Guangxi	24887	26073
	Tianjin	601	6052		Hainan	3020	5644
Northeast	Heilongjiang	32288	131734	Southwest	Chongqing	11160	26071
	Jilin	11216	64328		Guizhou	14247	34439
	Liaoning	9411	55105		Sichuan	42540	76425
East	Anhui	42952	36177		Tibet	186	4391
	Fujian	13950	6581		Yunnan	17243	50670
	Jiangsu	41065	25004	Northwest	Gansu	186	65075
	Jiangxi	32365	12229		Ningxia	4752	13137
	Shandong	1759	99375		Qinghai	0	8224
	Shanghai	3396	241		Shaanxi	8224	61423
	Zhejiang	21569	3122		Xinjiang	562	76549
Central	Henan	7595	98985	Total	Total	457488	1318081

In published studies, the emissions of atmospheric pollutants from crop residue burning were estimated based on statistical yearbook data or fire count data derived from satellite observations. Alternatively, in this study, we used land-cover data as activity data to calculate the pollutant emissions from crop residue burning. We therefore analyzed the correlation between the total area of sown crops determined from statistical data (China Bureau of Statistics) and farmland area determined from land-cover data. The results indicated a good correlation ($R^2 = 0.8044$; Fig. 2), confirming that our method was valid. Compared to other methods, the use of high-resolution activity data (paddy and nonirrigated farmland areas determined from land-cover data) improved the resolution of the inventory of pollutant emissions from crop residue burning.

2.4 Emission factors

Table 2 summarizes the emission factors used in this study for the burning of different types of crop straws. The emission factors were taken from MEE (2014). These emission factors are lower than those of Wang and Zhang (2008) and Qiu et al. (2016) but higher than those of Zhou et al. (2017). It would be useful to collect more local data in future studies.

2.5 Uncertainty analysis of atmospheric pollutant emissions

The Monte Carlo method (Cao et al., 2006; Zhang et al., 2009) was used to analyze the uncertainties in pollutant emissions from crop residue burning. These uncertainties were mainly introduced during the calculation process and originated from the activity data, emission factors, and other key parameters (e.g., the ratio of crop residue to production) (Cao et al., 2006; 2011; Zhang et al., 2009; Li et al., 2019). The uncertainty ranges in the emission estimates for different pollutants were obtained in the four following steps. First, we assumed that the uncertainties in the activity data, emission factors, and other key parameters could be described by normal or lognormal distributions. In this study, activity data were assumed to follow uniform distributions (Qiu et al., 2016), and emission factors were assumed to follow lognormal distributions (IPCC, 2011; Peng et al., 2016; Zhou et al., 2017). Second, we extracted the values of analogue activity data and emission factors data that fit

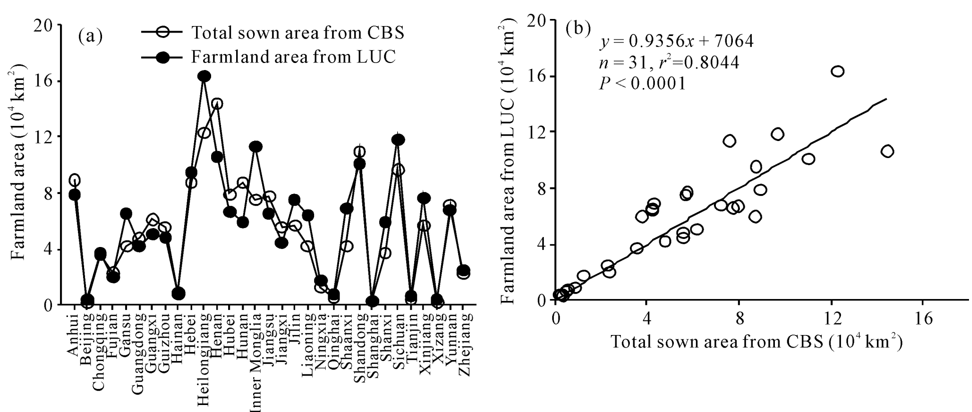

Fig. 2 Comparison of farmland area from LUC (land-cover change data) and CBS (China Bureau of Statistics) in different provinces in China, respectively (a) and regression analysis between total sown areas of crops from the CBS and farmland area from LUC (b) in 27 provinces and four municipalities in China in 2015

Table 2 Emission factors of atmospheric pollutants from crop residue burning

Type of crop	PM_{10} (g/kg)	$PM_{2.5}$ (g/kg)	VOCs (g/kg)	NH_3 (g/kg)	NO_x (g/kg)	SO_2 (g/kg)	CO (g/kg)
Wheat	11.95	11.71	10.4	0.68	4.3	0.44	53.0
Maize	7.73	7.58	7.48	0.37	3.31	0.85	59.6
Rice	5.78	5.67	8.45	0.53	1.42	0.53	27.7
Others	6.93	6.79	8.45	0.53	2.92	0.53	49.9

the normal or lognormal distribution. The numerical values of activity data, emission factors, or other key parameters were used to calculate the pollutant emissions based on the algorithms discussed in section 2.1. Third, we extracted the values of key parameters (e.g., activity data and emission factors) over 200 000 times to repeatedly calculate the pollutant emissions. Finally, the standard deviations of the resulting distributions were estimated with a 95% confidence interval.

3 Results

3.1 Levels of pollutant emissions from crop residue burning

Based on the land-cover change data, crop residue burning resulted in substantial emissions of atmospheric pollutants in 2015 (Table 3). The emissions of PM_{10}, $PM_{2.5}$, VOCs, NOx, SO_2, CO, and NH_3 from crop residue burning on nonirrigated farmland in 2015 were

Table 3 Particulate matter and gaseous emissions from nonirrigated farmland crop residue burning in China in 2015

Regions in China	Province	SO_2 (t)	NO_x (t)	NH_3 (t)	CO (t)	VOCs (t)	PM_{10} (t)	$PM_{2.5}$ (t)
North	Beijing	39	294	44	3972	704	789	774
	Hebei	1074	7457	1175	106604	18775	19548	19156
	Inner Mongolia	614	5109	824	67961	12775	13785	13508
	Shanxi	1266	9001	1436	125983	22834	24074	23593
	Tianjin	0	0	0	0	0	0	0
Northeast	Heilongjiang	1480	8428	1479	139582	23659	20395	19984
	Jilin	1756	12067	1836	170735	29658	31826	31190
	Liaoning	763	4298	609	65876	10370	10918	10701
East	Anhui	1844	15238	2417	201843	37653	41196	40369
	Fujian	129	712	120	11764	1945	1730	1695
	Jiangsu	1882	10555	1528	163268	25885	26702	26172
	Jiangxi	342	2131	321	31563	5276	5506	5396
	Shandong	6528	40926	5906	593396	98241	107043	104915
	Shanghai	0	0	0	0	0	0	0
	Zhejiang	229	1457	215	20942	3550	3851	3775
Central	Henan	2721	15454	2391	242252	39648	38912	38136
	Hubei	950	5850	879	87025	14491	15098	14797
	Hunan	709	5220	830	71604	13153	14104	13822
South	Guangdong	1024	7625	1158	103839	18496	20418	20009
	Guangxi	895	5802	854	83450	14046	15200	14897
	Hainan	4	22	4	375	64	52	51
Southwest	Chongqing	774	4064	851	61375	13498	12230	11989
	Guizhou	199	1342	236	18629	3715	3795	3720
	Sichuan	3150	17416	3017	264191	49256	47949	47001
	Tibet	0	0	0	0	0	0	0
	Yunnan	2549	16767	2620	236987	42466	45348	44446
Northwest	Gansu	683	5351	871	71924	13606	14585	14293
	Ningxia	313	2408	391	32704	6120	6519	6388
	Qinghai	144	928	132	13282	2200	2434	2385
	Shaanxi	719	5049	798	71062	12742	13442	13174
	Xinjiang	2590	19621	3152	267120	49607	53098	52036
Total		35372	230592	36092	3329309	584432	610545	598372

estimated to be 610.5, 598.4, 584.4, 230.6, 35.4, 3329.3, and 36.1 Gg, respectively. The emissions of particulate matter and gaseous pollutants were highest in east China, particularly in the provinces of Shandong, Henan, Anhui, Zhejiang, and Hunan. The emissions of PM_{10}, $PM_{2.5}$, VOCs, SO_2, NH_3, CO, and NO_x in east China accounted for 30.5%, 30.5%, 29.5%, 31.0%, 29.1%, 30.7%, and 30.8% of nationwide pollutant emissions from crop residue burning, respectively. In contrast, the emissions were lowest in south China, which contributed 5.8%, 5.8%, 5.6%, 5.4%, 5.6%, 5.6%, and 5.8% of total national pollutant emissions, respectively. Beijing, Tianjin, and Shanghai had relatively low levels of atmospheric pollutant emissions from crop residue burning on nonirrigated farmland due to their low levels of agricultural crop production and strict control policies for crop straw burning. The small percentage of crop straw burned in the fields of Inner Mongolia, where crop straws are mainly used in feed production for animal husbandry, led to low levels of atmospheric pollutant emissions from crop residue burning. The spatial patterns of emissions were similar for different atmospheric pollutants, with emission levels decreasing in the following order among the seven regions: East > Southwest > Northwest > Central > Northeast > North > South China.

Next, we estimated the emissions of particulate matter and gaseous pollutants from the burning of paddy rice straw in China in 2015 (Table 4). The burning of

Table 4 Particulate matter and gaseous emissions from paddy rice residue burning in China

Regions in China	Province	SO_2 (t)	NO_x (t)	NH_3 (t)	CO (t)	VOCs (t)	PM_{10} (t)	$PM_{2.5}$ (t)
North	Beijing	0	0	0	0	0	0	0
	Hebei	19	52	19	1007	307	210	206
	Inner Mongolia	0	0	0	6	2	1	1
	Shanxi	0	0	0	0	0	0	0
	Tianjin	0	0	0	0	0	0	0
Northeast	Heilongjiang	896	2399	896	46806	14278	9767	9581
	Jilin	217	583	217	11367	3467	2372	2327
	Liaoning	40	107	40	2079	634	434	426
East	Anhui	43	115	43	2252	687	470	461
	Fujian	386	1034	386	20161	6150	4207	4127
	Jiangsu	2711	7264	2711	141689	43223	29566	29003
	Jiangxi	2264	6067	2264	118345	36102	24694	24224
	Shandong	10	27	10	530	162	111	108
	Shanghai	0	0	0	0	0	0	0
	Zhejiang	1016	2723	1016	53114	16203	11083	10872
Central	Henan	369	988	369	19273	5879	4021	3945
	Hubei	1886	5054	1886	98583	30073	20571	20179
	Hunan	4605	12339	4605	240688	73423	50223	49267
South	Guangdong	1512	4050	1512	78998	24099	16484	16170
	Guangxi	1383	3707	1383	72307	22058	15088	14801
	Hainan	0	0	0	0	0	0	0
Southwest	Chongqing	446	1195	446	23310	7111	4864	4771
	Guizhou	108	290	108	5665	1728	1182	1159
	Sichuan	2480	6646	2480	129640	39547	27051	26536
	Tibet	0	0	0	0	0	0	0
	Yunnan	900	2412	900	47058	14355	9819	9632
Northwest	Gansu	0	0	0	0	0	0	0
	Ningxia	24	65	24	1262	385	263	258
	Qinghai	0	0	0	0	0	0	0
	Shaanxi	149	399	149	7777	2372	1623	1592
	Xinjiang	3	8	3	150	46	31	31
Total		21469	57521	21469	1122068	342291	234135	229680

paddy rice residue generated the emission of 234.1 Gg PM_{10}, 229.7 Gg $PM_{2.5}$, 342.3 Gg VOCs, 57.5 Gg NO_x, 57.5 Gg SO_2, 1122.1 Gg CO, and 21.5 Gg NH_3 in 2015. In contrast to the results obtained for nonirrigated farmland, the emissions of atmospheric pollutants from paddy rice straw burning were highest in east and central China (e.g., Hunan, Guangdong, Guangxi, Yunnan, and Jiangsu) and lowest in northwest and north China (e.g., Gansu and Tibet). This spatial distribution of emissions is related to the spatial distribution of paddy rice area sown in 2015. The emissions of atmospheric pollutants from paddy rice straw burning in central and east China accounted for 32.0% and 30.0% of all emissions from paddy rice straw burning in China, respectively; in contrast, northwest and north China accounted for only 0.8% and 0.1% of total emissions, respectively. Among the seven regions, the level of pollutant emissions from paddy rice straw burning decreased in the following order: central > east > southwest > south > northeast > northwest > north China.

3.2 Spatial distributions of pollutant emissions from crop straw burning

The spatial distributions of pollutant emissions (annual gridded emissions at a spatial resolution of 0.1° × 0.1°) from crop straw burning (including paddy rice and dryland crops) in China are shown in Fig. 3. The spatial emission patterns of the different atmospheric pollutants from crop residue burning were similar in 2015. Taking $PM_{2.5}$ as an example, the emissions from crop residue burning were highest over east and central China, particularly in Shandong, Jiangsu, Zhejiang, and Hunan provinces, which have large areas of nonirrigated and paddy farmland relative to other regions in China. In Shandong, Jiangsu, Zhejiang, and Hunan provinces, the annual maximum emission of $PM_{2.5}$ from crop residue burning exceeded 16 930 kg in each grid. Lower emission levels of less than 1000 kg/yr in each grid were observed in Beijing, Tianjin, Guizhou, Qinghai, and Tibet. These lower emissions can be attributed to the severe restrictions on open straw burning, high utilization rates of crop residues, and/or relatively small areas of nonirrigated farmland and paddy land in these regions. In most provinces, the average emissions of $PM_{2.5}$ from crop residue burning ranged from 2000–26 000 kg/grid. The mean annual emissions of $PM_{2.5}$ were 454.0 kg/km^2 for the burning of dryland crop (e.g., rice, wheat, and maize) residues and 502 kg/km^2 for paddy rice straw burning.

For PM_{10}, the national average emissions in 2015 were 463.2 and 511.8 kg/km^2 for the burning of dryland crop straw and paddy rice straw, respectively; the corresponding values for CO were 2525 and 2453 kg/km^2, respectively, while those for VOCs were 443.4 and 748.2 kg/km^2, respectively. The annual emissions of SO_2, NH_3, and NO_x were smaller than those of PM_{10}, $PM_{2.5}$, and VOCs, which was attributed to their smaller emission factors. The average annual emissions of SO_2, NH_3, and NO_x for paddy rice straw were 46.9, 46.9, and 125.7 kg/km^2, respectively. The annual emissions of SO_2, NH_3, and NO_x for dryland crop straw burning were 26.8, 27.4, and 174.9 kg/km^2, respectively.

3.3 Temporal distributions of pollutant emissions from crop straw burning

The temporal distributions of the emissions of different pollutants from crop residue burning were similar in China in 2015. Taking $PM_{2.5}$ as an example, the monthly contributions of $PM_{2.5}$ emissions to annual $PM_{2.5}$ emissions are shown in Fig. 3 to demonstrate the temporal distributions of atmospheric pollutant emissions from crop residue burning. The emissions of atmospheric pollutants exhibited similar monthly variations in different regions, with maximum values observed in October in North, Northeast, Northwest, East, and Southwest China and in June and July in other regions (central and South China). In North China, the emission peaks of $PM_{2.5}$ observed in June (16.9% of total annual $PM_{2.5}$ emissions) and October (80.6%) were related to the burning of both paddy rice and dryland crop straw. These peaks correspond to the harvest season, and winter wheat straw was mainly burned in June. In northeast China, the highest $PM_{2.5}$ emissions were observed in September (43.2%) and October (56.3%), when the crop straw was cleared. Mainly maize straw and soybean straw were burned in October, while rice straw was burned in September after harvesting. In Northwest China, June, September, and October accounted for 10.5%, 30.9%, and 42.6% of annual $PM_{2.5}$ emissions, respectively. The crop of winter wheat was burned in June; maize, rice, and soybean straws were burned in September and October; and cotton straw was burned in November. These crops straw contributions highlight the outdoor burning patterns in northwest China. Secondary peaks in $PM_{2.5}$ emissions were found in May (15.1%) and October (72.8%) and primary peak of the annual from crop residue burning in southwest China. May is the most important month for harvesting wheat and maize, and rice straw was mainly burned in October. In central and south China, the largest $PM_{2.5}$ emissions were observed in June and July, which accounted for 43.5% and 54.2% of annual $PM_{2.5}$ emissions, respectively. A secondary peak was observed in October, when high emissions occurred in regions with double-season crop systems. While east China also has a double-season crop system, the $PM_{2.5}$ emissions peaked in October (42.0%) with a second peak in June (38.2%). The $PM_{2.5}$ emissions in June were dominated by the burning of winter-wheat straw, while those in October were dominated by the burning of maize, rice, and soybean straw.

Fig. 4b shows strong seasonal variations in the emissions of atmospheric pollutants from crop residue burning. Emissions were highest in October followed by June. The monthly variability in $PM_{2.5}$ emissions from crop residue burning is controlled by the seasonal operations involved in harvesting different crops.

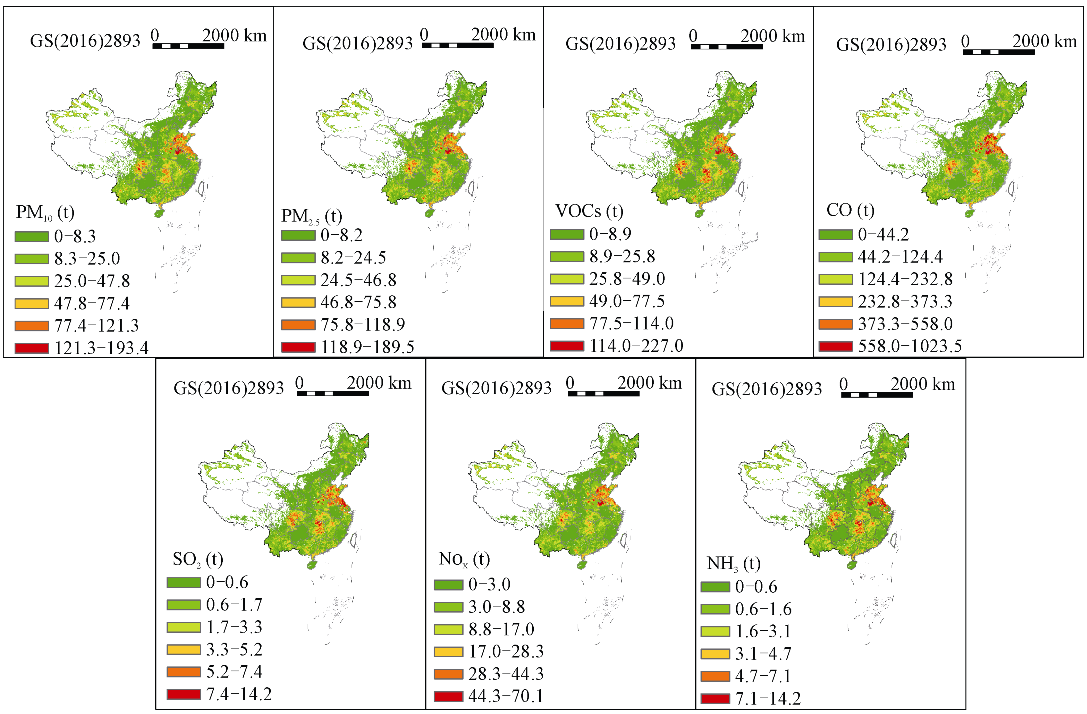

Fig. 3 The spatial distribution of (a) PM_{10}, (b) $PM_{2.5}$, (c) VOCs, (d) CO, (e) SO_2, (f) NO_x, and (g) NH_3 of crop residue burning in China (0.1° × 0.1°)

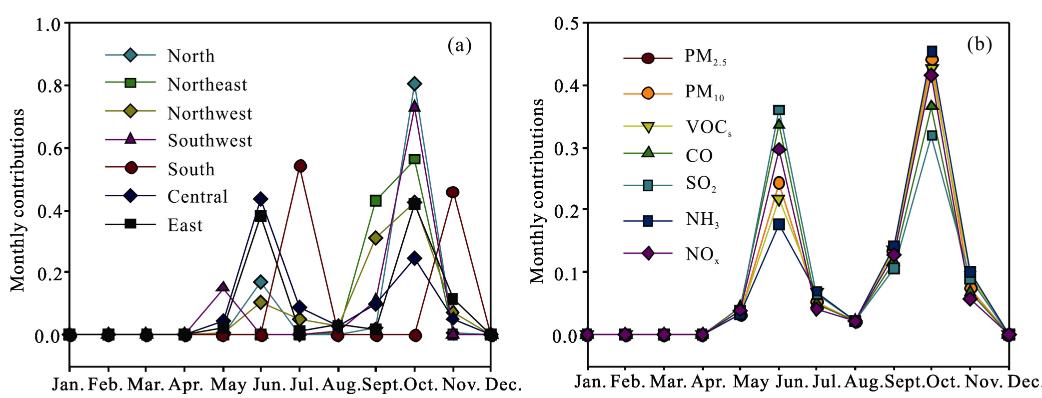

Fig. 4 Monthly contributions of atmospheric pollutant emissions in seven regions (a) and whole China (b)

3.4 Uncertainties in estimates of emissions from crop residue burning

We ran 200 000 Monte Carlo simulations to estimate the range of emissions. The resulting uncertainty ranges are shown in Table 5. The uncertainties ranges of atmospheric pollutants in the estimated emissions (min, max) (95% confidence intervals) of $PM_{2.5}$, PM_{10}, VOCs, NH_3, NO_x, SO_2, and CO were (21.9%, 106.4%), (2.5%, 71.1%), (3.7%, 73.2%), (32.8%, 121.9%), (−10.1%, 49.9%), (−12.8%, 45.6%), and (−10.9%, 48.6%), respectively. The main source of these uncertainties was the emission factors rather than the agricultural activity data from statistical yearbooks.

The uncertainty ranges for $PM_{2.5}$, PM_{10}, VOCs, and NH_3 emissions were similar (minimum and maximum uncertainty were both larger than 0%), while the uncertainty ranges of NO_x, SO_2, and CO were similar (minimum < 0 and maximum > 0). This can be explained by the emission factors used in the estimations, which were much lower than ($PM_{2.5}$, PM_{10}, VOCs, NH_3) or similar to (NO_x, SO_2, and CO) the average values of emission factors used in published studies.

4 Discussion

Currently, the large amount of crop production coupled with a lack of effective emission control strategies for open biomass burning in China has led to the large-scale burning of crop straw in open fields during harvest periods. An accurate inventory of atmospheric pollutants emitted by crop residue burning is necessary to understand, predict, and control the effects of agricultural emissions on air quality and human health. However, past estimates of atmospheric pollutant emissions from crop residue burning were developed based on statistical yearbook data, which generally have low resolution (province- or city-level resolution). In this study, we developed a high-resolution inventory of emissions from crop residue burning based on high-resolution land-cover data (1 km × 1 km) from satellite observations and county-level burned cropland area data. Data on land-cover change in China can generally be obtained easier than fire count data and are more accurate than statistical data. The emission inventory developed in this study based on land-cover change data has a higher resolution than previously reported inventories.

The spatial variations in atmospheric pollutant emissions from crop residue burning in 2015 were related to the spatial distributions of farmland area in China, including paddy and nonirrigated farmland area. The highest emissions from burning paddy rice straw were found in central and east China (e.g., Hunan, Jiangsu, Sichuan, and Jiangxi provinces), where large areas of sown paddy land were found in 2015. The highest emissions from burning dryland straw were found in east and southwest China (e.g., Shandong and Sichuan provinces) due to the large areas of nonirrigated farmland and the production of abundant straw resources in these regions. Control policies for crop straw burning also affected the spatial variations in the emissions of atmospheric pollutants from crop residue burning. Such policies resulted in lower emissions from crop residue burning in nonirrigated farmland in Beijing, Tianjin, and Shanghai. The monthly variability in pollutant emissions was controlled by the seasonal agricultural operations of different crop types and cropping systems in different regions. The uncertainties in the estimated emissions of different pollutants from crop residue burning were also calculated in this study. Uncertainty is a critical factor in verifying the accuracy of inventories of agricultural emissions. The range of uncertainty in our emissions estimates was as high as −12.8% to 106.4%; however, this range is smaller than those reported in many previous studies. The estimates in this

Table 5 Uncertainty ranges of atmospheric pollutant in emission estimates (min, max) in this study and other references (95% confidence intervals) (%)

SO_2	$PM_{2.5}$	PM_{10}	VOCs	NH_3	NO_x	CO	Reference
(–71, 304)	(–60, 83)	–	(–67, 94)	–	(–49, 78)	(–91, 155)	Peng et al., 2016
(–76, 75)	(–54, 34)	(–37, 80)	(–55, 21)	(–78, 76)	(–62, 24)	(–41, 47)	Zhou et al., 2017
(–47, 121)	(–77, 213)	(–77, 213)	(–72, 213)	(–24, 78)	(–36, 92)	(–61, 152)	Qiu et al., 2016
–	(–62.5, 105.1)	–	–	–	–	–	Li et al., 2019
(–12.8, 45.6)	(21.9, 106.4)	(2.5, 71.1)	(3.7, 73.2)	(32.8, 121.9)	(–10.1, 49.9)	(–10.9, 48.6)	This study

study were improved by the use of higher-quality activity data. The uncertainty was primarily introduced by the nonlocally derived emission factors.

The cross-examination of atmospheric pollutant emissions between different inventories is important to verify the accuracy of emission inventories. We compared the atmospheric pollutant emissions and their spatiotemporal distributions compiled in this study with those reported by Peng et al. (2016) for the year 2009 and Qiu et al. (2016) for the year 2013 along with the EDGAR emission inventories (Emissions Database for Global Atmospheric Research) (Fig. 5).

Peng et al. (2016) used a bottom-up approach, while Qiu et al. (2016) use a top-down approach to compile the inventories. The emissions of pollutants from crop burning estimated in this study generally were lower than the estimates reported by Peng et al. (2016) and Qiu et al. (2016), and the spatial distributions were similar. The differences can be attributed to the different estimation methods, emission factors, and activity data. The emission factors for burned rice, maize, and cotton straw used in Peng et al. (2016) were higher than the values adopted in our study. The lower ratios of crop residue to production and crop yields used in Peng et al.

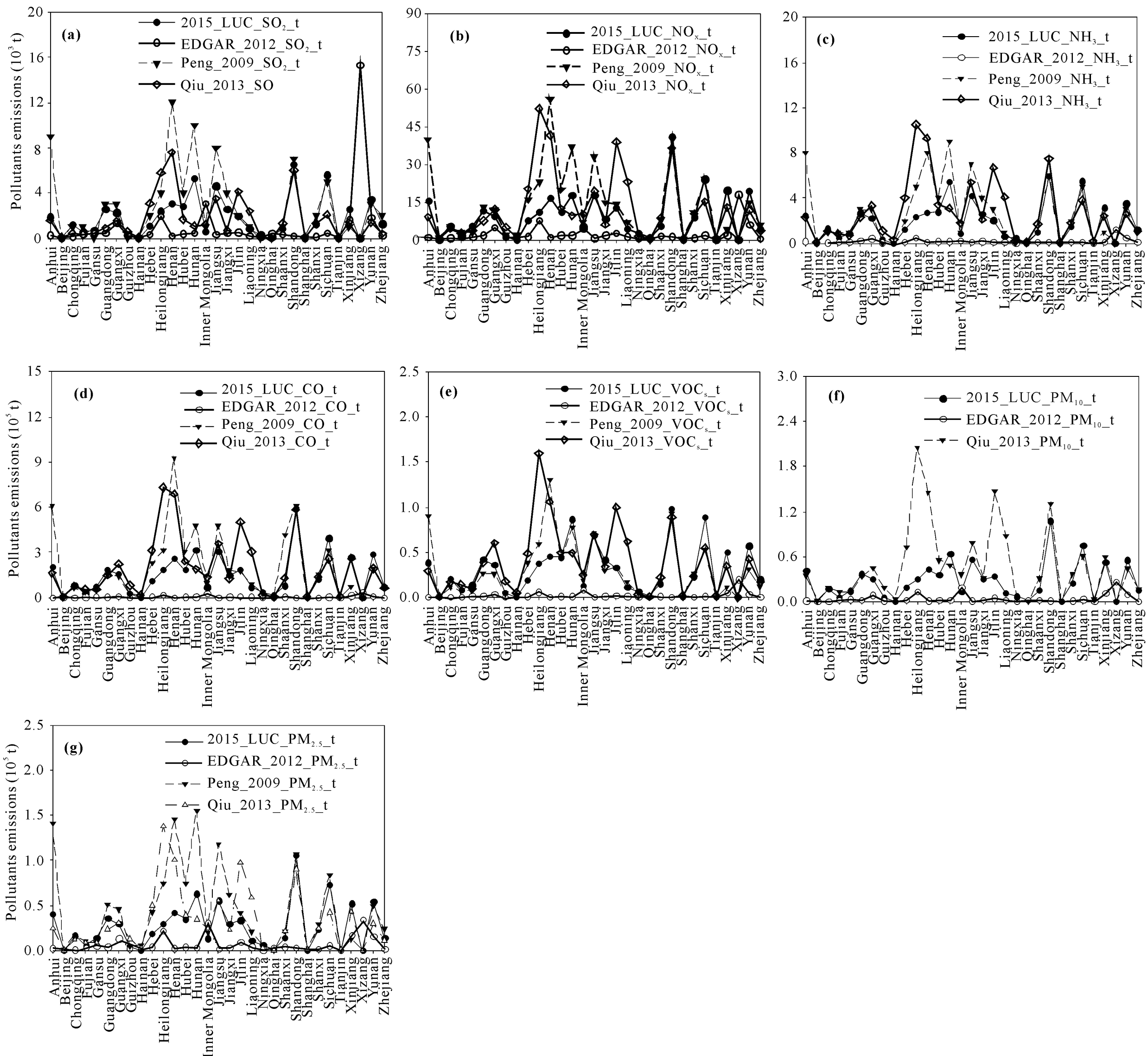

Fig. 5 Comparison of atmospheric pollutant emissions and their spatial distributions in this study with published emission inventories: (a) SO_2, (b) NO_x, (c) NH_3, (d) CO, (e) VOCs, (f) PM_{10}, and (g) $PM_{2.5}$. 2015_LUC: data from this study; EDGAR_2012: data from EDGAR; Peng_2009: data from Peng et al. (2016); Qiu_2013: data from Qiu et al. (2016)

(2016) did not contribute significantly to the difference between the findings of this study and their results. Comparing the estimated atmospheric pollutant emissions and their spatiotemporal distributions obtained in our study and by Qiu et al. (2016) confirmed the validity of our results. The agricultural activity data used in Qiu et al. were fire count data based on satellite observations, while land-cover data from remote sensing served as the activity data in our study. The emissions of atmospheric pollutants from crop residue burning in EDGAR (Crippa et al., 2018) are lower than those in 2015_LUC (the emission inventory of crop residue burning in China in 2015 that used satellite-retrieved land-cover data as activity data to be compiled). The emissions of particulate and gaseous pollutants from straw combustion between EDGAR and 2015_LUC exhibited significant differences in Inner Mongolia and Tibet, with EDGAR predicting higher pollutant emissions in those regions.

5 Conclusions

The burning of crop residues contributes to the emissions of large quantities of atmospheric aerosols. However, existing inventories of atmospheric pollutant emissions from crop residue burning based on statistical data have low resolution because county-level activity data cannot be obtained directly from statistical yearbooks. Emission inventories based on fire count data derived from satellite observations generally have high uncertainty because of their limited resolution, missing data for small fires, and the lack of localized vegetation data. To improve the resolution and accuracy of inventories of agricultural emissions, we extracted paddy and nonirrigated farmland areas from remote sensing land-cover data (http://www.resdc.cn/data.aspx?DATAID=184) and used them to develop a high- resolution inventory of emissions from crop residue burning.

The emissions of PM_{10}, $PM_{2.5}$, VOC_s, NO_x, SO_2, CO, and NH_3 from crop residue burning in nonirrigated farmland in China in 2015 were 610.5, 598.4, 584.4, 230.6, 35.4, 3329.3, and 36.1 Gg, respectively; the corresponding values for paddy rice residue burning were 234.1, 229.7, 342.3, 57.5, 57.5, 1122.1, and 21.5 Gg, respectively. The atmospheric pollutant emissions resulting from the burning of dryland crop residues were highest in east and central China, particularly in Shandong, Jiangsu, Zhejiang, and Hunan provinces. For paddy rice straw burning, the atmospheric pollutant emissions were highest in south and central China, including Hunan, Guangdong, Guangxi, Yunnan, and Jiangsu provinces. The emissions of different atmospheric pollutants showed similar monthly variations among different regions, with maximum emissions observed in October in north, northeast, northwest, east, and southwest China and in June and July in other regions (central and south China).

The findings indicate that crop residue burning emits a large quantity of atmospheric pollutants during the harvesting season. Thus, it is necessary to manage crop residue burning more effectively during severe haze events. Further research is needed to improve agricultural inventories through improvements in key data inputs. For example, the percentage of crop straw burned in the field, which may vary over time and space, needs further study.

Acknowledgement

We thank the Resource and Environment Data Cloud Platform of the Institute of Geographic Sciences and Natural Resources Research, Chinese Academy of Sciences which provided us with land-cover data for China (available at http://www.resdc.cn/). The provincial agricultural activity data used in this study are national data maintained by the National Bureau of Statistics of China (available at http://data.stats.gov.cn/easyquery.htm?cn=E0103).

References

Anhui Bureau of Statistics (ABS), Anhui Survey Team of National Bureau of Statistics, 2016. *Anhui Statistical Yearbook*. Beijing: China Statistics Press. (in Chinese)

Beijing Bureau of Statistics (BBS), 2016. *Beijing Statistical Yearbook*. Beijing: China Statistics Press. (in Chinese)

Cao Guoliang, Zhang Xiaoye, Zheng Fangcheng et al., 2006. Estimating the quantity of crop residues burnt in open field in China. *Resources Science*, 28(1): 9–13. (in Chinese)

Cao G L, Zhang X Y, Gong S L et al., 2011. Emission inventories of primary particles and pollutant gases for China. *Chinese Science Bulletin*, 56(8): 781. doi: 10.1007/s11434-011-4373-7

Chongqing Bureau of Statistics (CBS), 2016. *Chongqing Statistical Yearbook*. Beijing: China Statistics Press. (in Chinese)

Crippa M, Guizzardi D, Muntean M et al., 2018. Gridded emissions of air pollutants for the period 1970–2012 within EDGAR v4.3.2. *Earth System Science Data*, 10(4):

1987–2013. doi: 10.5194/essd-10-1987-2018

European Enviromental Agency (EEA), 2007. *EMEP/CORINAIR Emission Inventory Guidebook*: 2007. Technical Report No 16/2007.

Fujian Bureau of Statistics (FBS), Fujian Survey Team of National Bureau of Statistics, 2016. *Fujian Statistical Yearbook*. Beijing: China Statistics Press. (in Chinese)

Guangdong Bureau of Statistics (GDBS), Guangdong Survey Team of National Bureau of Statistics, 2016. *Guangdong Statistical Yearbook*. Beijing: China Statistics Press. (in Chinese)

Guangxi Bureau of Statistics (GXBS), 2016. *Guangxi Statistical Yearbook*. Beijing: China Statistics Press. (in Chinese)

Gansu Bureau of Statistics (GSBS), 2016. *Gansu Statistical Yearbook*. Beijing: China Statistics Press. (in Chinese)

Guizhou Bureau of Statistics (GZBS), Guizhou Survey Team of National Bureau of Statistics, 2016. *Guizhou Statistical Yearbook*. Beijing: China Statistics Press. (in Chinese)

Hainan Bureau of Statistics (HBS), Hainan Survey Team of National Bureau of Statistics, 2016. *Hainan Statistical Yearbook*. Beijing: China Statistics Press. (in Chinese)

He Hong, Wang Xinming, Wang Yuesi, et al., 2013. Formation mechanism and control strategies of haze in China. *Bulletin of Chinese Academy of Sciences*, 28(3): 344–352. (in Chinese)

Hebei Bureau of Statistics (HBBS), 2016. *Hebei Economic Yearbook*. Beijing: China Statistics Press. (in Chinese)

Heilongjiang Bureau of Statistics (HLJBS), 2016. *Heilongjiang Statistical Yearbook*. Beijing: China Statistics Press. (in Chinese)

Henan Bureau of Statistics (HNBS), 2016. *Henan Statistical Yearbook*. Beijing: China Statistics Press. (in Chinese)

Hubei Bureau of Statistics (HUBBS), Hubei Survey Team of National Bureau of Statistics, 2016. *Hubei Statistical Yearbook*. Beijing: China Statistics Press. (in Chinese)

Hunan Bureau of Statistics (HUNBS), 2016. *Hunan Statistical Yearbook*. Beijing: China Statistics Press. (in Chinese)

Inner Mongolia Bureau of Statistics (IMBS), 2016. *Inner Mongolia Statistical Yearbook*. Beijing: China Statistics Press. (in Chinese)

IPCC (The Intergovernmental Panel on Climate Change), 2011. The Intergovernmental Panel on Climate Change (IPCC): Climate Change 2007. Available at: http://www.ipcc.ch

Jiangsu Bureau of Statistics (JSBS), 2016. *Jiangsu Statistical Yearbook*. Beijing: China Statistics Press. (in Chinese)

Jiangxi Bureau of Statistics (JXBS), Jiangxi Survey Team of National Bureau of Statistics, 2016. *Jiangxi Statistical Yearbook*. Beijing: China Statistics Press. (in Chinese)

Jilin Bureau of Statistics (JLBS), 2016. *Jilin Statistical Yearbook*. Beijing: China Statistics Press. (in Chinese)

Li R M, Chen W W, Xiu A J et al., 2019. A comprehensive inventory of agricultural atmospheric particulate matters (PM_{10} and $PM_{2.5}$) and gaseous pollutants (VOCs, SO_2, NH_3, CO, NO_x and HC) emissions in China. *Ecological Indicators*, 107: 105609.

Liaoning Bureau of Statistics (LBS), 2016. *Liaoning Statistical Yearbook*. Beijing: China Statistics Press. (in Chinese)

MEE, 2014. *Technical Guidelines on Emission Inventory Development of Air Pollutants from Biomass Burning* (*on Trial*). Ministry of Ecology and Environmental Protection of the People's Republic China. Available at: http://www.mee.gov.cn/gkml/hbb/bgg/201501/t20150107_293955.htm

National Bureau of Statistics of China (NBSC), 2016a. *China Statistical Yearbook* (*County-level*) 2016. Beijing: China Statistics Press. (in Chinese).

National Bureau of Statistics of China (NBSC), 2016b. *China Statistical Yearbook 2016*. Beijing: China Statistics Press. (in Chinese).

Ningxia Bureau of Statistics (NBS), Ningxia Survey Team of National Bureau of Statistics, 2016. *Ningxia Statistical Yearbook*. Beijing: China Statistics Press. (in Chinese)

Peng Liqun, Zhang Qiang, He Kebin, 2016. Emissions inventory of atmospheric pollutants from open burning of crop residues in China based on a national questionnaire. *Research of Environmental Sciences*, 29(8): 1109–1118. (in Chinese)

Qinghai Bureau of Statistics (QBS), Qinghai Survey Team of National Bureau of Statistics, 2016. *Qinghai Statistical Yearbook*. Beijing: China Statistics Press. (in Chinese)

Qiu X H, Duan L, Chai F H et al., 2016. Deriving high-resolution emission inventory of open biomass burning in China based on satellite observations. *Environmental Science & Technology*, 50(21): 11779–11786. doi: 10.1021/acs.est.6b02705

Shaanxi Bureau of Statistics (SBS), 2016. *Shaanxi Statistical Yearbook*. Beijing: China Statistics Press. (in Chinese)

Shandong Bureau of Statistics (SDBS), 2016. *Shandong Statistical Yearbook*. Beijing: China Statistics Press. (in Chinese)

Shanghai Bureau of Statistics (SHBS), 2016. *Shanghai Statistical Yearbook*. Beijing: China Statistics Press. (in Chinese)

Shanxi Bureau of Statistics (SXBS), 2016. *Shanxi Statistical Yearbook*. Beijing: China Statistics Press. (in Chinese)

Sichuan Bureau of Statistics (SCBS), 2016. *Sichuan Statistical Yearbook*. Beijing: China Statistics Press. (in Chinese)

Tianjin Bureau of Statistics (TJBS), Tianjin Survey Team of National Bureau of Statistics, 2016. *Tianjin Statistical Yearbook*. Beijing: China Statistics Press. (in Chinese)

Tibet Bureau of Statistics (TBS), Tibe Survey Team of National Bureau of Statistics, 2016. *Tibet Bureau of Statistics*. Beijing: China Statistics Press. (in Chinese)

Wang Shuixiao, Zhang Chuying, 2008. Spatial and temporal distribution of air pollutant emissions from open burning of crop residues in China. *Sciencepaper Online*, 3(5): 329–333. (in Chinese)

Wu J, Kong S F, Wu F Q et al, 2018. Estimating the open biomass burning emissions in central and eastern China from 2003 to 2015 based on satellite observation. *Atmospheric Chemistry and Physics*, 18(16): 11623–11646. doi: 10.5194/acp-18-11623-2018

Xinjiang Bureau of Statistics (XBS), 2016. *Xinjiang Statistical Yearbook*. Beijing: China Statistics Press. (in Chinese)

Yunnan Bureau of Statistics (YBS), 2016. *Yunan Statistical Yearbook*. Beijing: China Statistics Press. (in Chinese)

Zhang Qiang, Klimont Z, Streets D G et al., 2006. Emission model of anthropogenic sources and estimation of emission inventory in 2001, China. *Progress in Natural Science*, 16(2): 223–231. (in Chinese)

Zhang Q, Streets D G, Carmichael G R et al., 2009. Asian emissions in 2006 for the NASA INTEX-B mission. *Atmospheric Chemistry and Physics*, 9(14): 5131–5153. doi: 10.5194/acp-9-5131-2009

Zhejiang Bureau of Statistics (ZBS), 2016. *Zhejiang Statistical Yearbook*. Beijing: China Statistics Press. (in Chinese)

Zhou Y, Xing X F, Lang J L et al., 2017. A comprehensive biomass burning emission inventory with high spatial and temporal resolution in China. *Atmospheric Chemistry and Physics*, 17(4): 2839–2864. doi: 10.5194/acp-17-2839-2017